ELSEVIER

Time-dependence of nuclear magnetic resonance quadrupole interactions for polymers under shear

J.M. Atkin, R.J. Cormier, P.T. Callaghan*

MacDiarmid Institute for Advanced Materials and Nanotechnology, School of Chemical and Physical Sciences, Victoria University of Wellington, New Zealand

Abstract

We consider the problem of performing NMR spectroscopy under conditions of flow, a central issue in Rheo-NMR. By way of example, the effects of rotational motion on the deuterium NMR spectrum are considered for Couette cell experiments involving deformation of polymers under shearing conditions. The polymer was modelled as a power law fluid and for each streamline, the spin Hamiltonian evolved to allow for flow reorientation. The gap-integral spectra are compared with the 'ideal' spectra for a polymer under shear, but without reorientation. It is found that flow does affect the shape of the deuterium spectra, as well as slightly perturbing the splittings.
© 2004 Elsevier Inc. All rights reserved.

1. Introduction

One of many recent applications [1–6] of magnetic resonance is its use in rheology, the science of flow. A central question in rheology concerns the molecular basis of complex visco-elasticity in non-Newtonian liquids. NMR offers the particular advantage that is able, through magnetic resonance imaging, to provide a map of the flow field, thus allowing the experimenter to know the velocity (and, crucially, its gradient) at every point in the fluid. But more importantly, NMR is a powerful tool for the investigation of molecular organisation and dynamics, through measurements of inter-nuclear dipolar interactions, nuclear quadrupole interactions, spin relaxation rates, and molecular self-diffusion coefficients. It is this diversity of approach which has given impetus to the emerging science of "Rheo-NMR" [4,5].

An intriguing aspect of Rheo-NMR is that one is generally called upon to perform NMR spectroscopy in a moving fluid. Such motion clearly complicates, but does not make impossible, self-diffusion measurements [2]. It may also complicate some forms of spectroscopy. In particular, if one is using the nuclear quadrupole interaction to yield information about molecular alignment in non-Newtonian liquids under shear or extensional flow [3,7–10,12–15], then the movement of the fluid may induce reorientations which shift the projected value of the quadrupole Hamiltonian, when measured in the zeroth order Zeeman frame of the magnetic field. It has emerged that the use of deuterium quadrupole interactions to measure shear and extension-induced order, has placed NMR in a leading position with respect to other techniques, such as neutron scattering and optical birefringence measurement, to the extent that magnetic resonance should become the definitive tool in Rheo-molecular investigation of flow-induced alignment. That being the case, it is reasonable to address the question as to whether flow itself

---
* Corresponding author. Fax: +646 350 5164.
  E-mail address: Paul.Callaghan@vuw.ac.nz (P.T. Callaghan).

may perturb the measurement of quadrupole interactions, and so complicate the interpretation of these experiments.

This paper examines one such example, namely that of cylindrical Couette flow. This approach has proven of some value in elucidating the precise details of shear-induced deformation of both polymers [8,9,12,13] and wormlike micelles [10,16,17]. While we focus here on a particular example, we would argue that the methodology we present does present a recipe for dealing with other closely related flow-perturbation difficulties in Rheo-NMR spectroscopy. The essential problem is that flow may cause a reorientation of molecules with respect to the Zeeman field. We will show here, by accounting for the contribution from each streamline, and then allowing the spin Hamiltonian to evolve in real time, that it is possible to reconstruct the signal and to test whether flow-induced perturbations are problematic.

We focus in particular on the measurement of the molecular deformation of an entangled polymer melt in shear. The deformation of the polymer can be described theoretically using the Doi–Edwards model [18,19], the alignment tensor being defined as:

$$S_{\alpha\beta} = \langle u_\alpha u_\beta - \tfrac{1}{3}\delta_{\alpha\beta}\rangle, \tag{1}$$

where the ensemble average is taken over all polymer segments, the **u** being tangent vectors to the polymer and α and β being chosen from the directions X, Y, and Z. The natural axis system is the hydrodynamic frame, where X is the velocity (**v**) direction, Y is the velocity gradient ($\nabla\mathbf{v}$), and Z is the vorticity ($\nabla \times \mathbf{v}$) direction. In the Doi–Edwards model, $S_{\alpha\beta}$ is directly calculable in terms of the parameter $\dot\gamma\tau_d$, where $\dot\gamma$ is the shear rate, $\partial v_X/\partial Y$ and τ_d is the polymer tube disengagement time. A plot of the alignment tensor components is shown in Fig. 1.

The experiment [9,12,13] employs the Couette cells shown in Fig. 2. The essential idea is to introduce a deuterated "spy molecule" into the polymer melt so that by rapid diffusion involving multiple collisions with the polymer, each imparting a favoured orientation due to steric hindrance, a motionally averaged "memory" of the polymer segmental orientation results. While the absolute magnitude of the quadrupole interaction is unknown, its dependence on shear rate, and in particular, its dependence on orientation of the hydrodynamic axes with respect to the Zeeman field, allows one to measure the full alignment tensor of the polymer, to within an arbitrary common constant. The trick, in the NMR experiment, is to correctly orient the cell and to use combinations of shaped RF pulses and magnetic field gradients [20] to select the desired region of fluid where the hydrodynamic axes have a chosen alignment with the magnetic field direction, z. Technical details of this experiment are given elsewhere [9,12,13,20]. Clearly, in
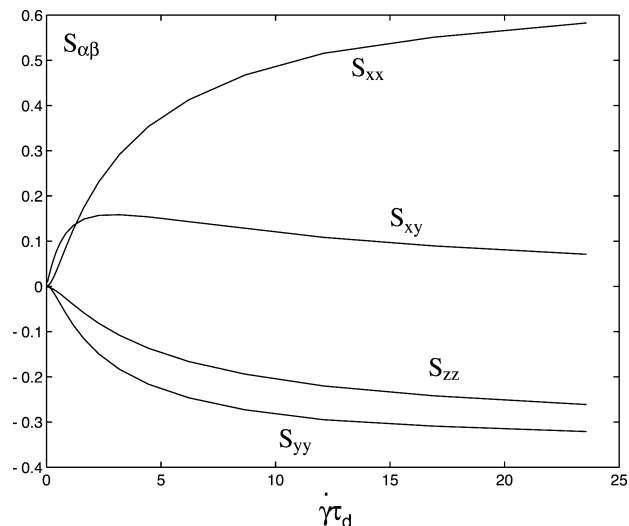

Fig. 1. Elements of Doi–Edwards alignment tensor for entangled polymer melt, as a function of the dimensionless shear rate (Deborah number), $\dot\gamma\tau_d$.
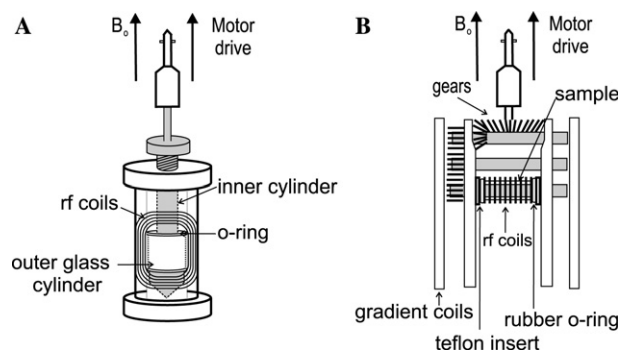

Fig. 2. Rheo-NMR cells used to shear a polydimethylsiloxane polymer melt (molecular weight 670 kDa) where in (A) the vorticity axis is collinear with the magnetic field while in (B) it is transverse to the magnetic field, allowing the velocity-gradient elements of the alignment tensor to be measured.

the case of vorticity axis selection, one may use a Couette cell whose rotation axis is colinear with the magnetic field. In this case azimuthal flow around that axis has no influence on the relevant orientation during measurement of the alignment tensor element, S_{ZZ}. However, in order to measure S_{XX}, S_{YY}, and S_{XY}, we must employ a cylindrical Couette cell for which the rotation axis is transverse to the applied magnetic field. The projection of the hydrodynamic tensor in the Zeeman frame is shown, schematically, in Fig. 3. By selective excitation, we may carry out a measurement of the deuterium quadrupole splitting at any chosen azimuthal orientation, Φ, an image obtained after such selection being also shown in Fig. 4.

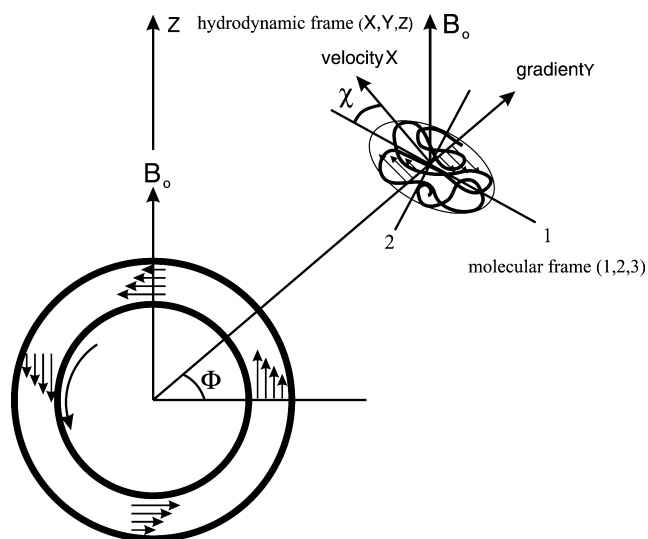To relate the predictions of the Doi–Edwards model to the NMR quadrupole interaction, it is necessary to

Fig. 3. Schematic showing the relative orientations of the hydrodynamic (X, Y, Z) axes with the transverse Couette cell axes. Note that the molecular $(1, 2, 3)$ frame has a principal axis which subtends an angle χ with the velocity direction. χ is known as the "extinction angle" in connection with birefringence measurements.
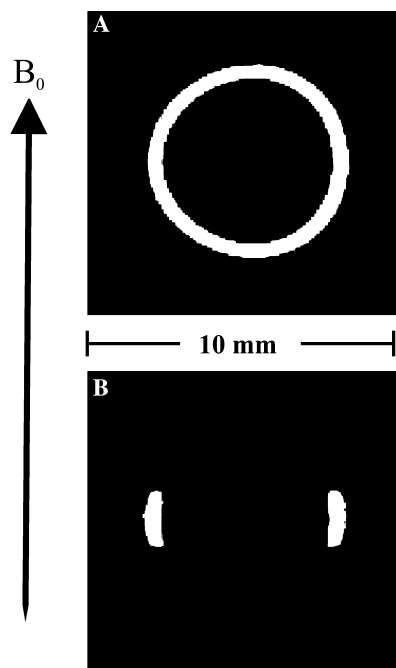

Fig. 4. NMR images of the polydimethylsiloxane situated in the annulus between the 2.5 mm radius inner cylinder (rotor) and 3 mm radius outer cylinder (stator). Note that the distortion is caused by diamagnetic susceptibility differences. In (A) the entire sample is shown whereas in (B) a selective excitation has preceded the imaging sequence so as to excite only the sample in the region of interest where the velocity direction is parallel to the magnetic field. This would correspond to a measurement of the element S_{XX}.

rotate this tensor to the frame of the applied magnetic field. Φ defines the orientations of X, Y, and Z with respect to B_0, so that

$$
S_{zz} = \begin{pmatrix} 1 & 0 & 0 \end{pmatrix} R(\Phi) \begin{pmatrix} S_{XX} & S_{XY} & 0 \\ S_{XY} & S_{YY} & 0 \\ 0 & 0 & S_{ZZ} \end{pmatrix} R^{-1}(\Phi) \begin{pmatrix} 1 \\ 0 \\ 0 \end{pmatrix}
$$
$$
= S_{XX} \cos^2 \Phi - 2 S_{XY} \sin \Phi \cos \Phi + S_{YY} \sin^2 \Phi.
$$
$$\tag{2}$$

Of course, during the time taken to acquire the signal from which the deuterium quadrupole spectrum may be derived, the fluid is moving, so that Φ is a time-dependent variable. Near the outer wall of the cell, where the velocity is close to zero, very little perturbation occurs. But near the inner wall, the flow-induced reorientation effect may be substantial. In the measurements previously reported, no account was made of this effect. The question arises therefore, is it a problem and, if so, what are the methods needed so that Rheo-NMR spectroscopy experiments may be performed with proper accuracy? Obviously there is a matter of comparative timescales. If the characteristic time associated with the spectral feature (for example the inverse of the splitting) is long compared with the rotation period of the inner cylinder, then a serious difficulty arises. One can imagine situations, for example when the flow is rapid and the spectral feature delicate, where such a problem is unavoidable. We note here that in our earlier experiments the spectral time was of the order of tens of milliseconds while the rotation periods were of the order of seconds, and it was on this basis that we held confidence in our measurements. Nonetheless, in that work, some intriguing spectral features arose which we were unable to explain. Further, the question of flow perturbations should not be lightly dismissed with arguments about timescales, but rather, it is worthy of proper, quantitative, investigation.

In seeking to understand this problem we point out the great advantage of Rheo-NMR methodology in that the flow field is inherently measurable [21] and indeed was measured in our prior work. Armed with a knowledge of the flow, there is nothing to prevent us from estimating its effect. This paper reports on a numerical simulation, in which we compare our results with experiment, finally concluding that while our previous measurements and their interpretation were justified, some care is needed in any such measurement where relative timescales might be unfavourable.

Our work concerns the spin-one deuterium nucleus which experiences an electric quadrupole interaction between the nuclear quadrupole moment and the surrounding electric field gradient, a gradient whose principal axes are embedded in the deuteron-containing molecular bond. In reiteration, this interaction is experienced in the presence of a much larger Zeeman interaction between the magnetic dipole moment and the polarising magnetic field B_0, and is therefore a first-order projection along the spin quantisation axis defined by the static magnetic field, z. The total Hamiltonian for this system

is $\mathcal{H} = -\omega I_z + P[I_z^2 - \frac{1}{3}I(I+1)]$, where P is a constant representing the size of the quadrupole interaction. However, the effect of the Zeeman term, and its inhomogeneity, can be cancelled by using an echo sequence which leads to a change in sign of the linear term whilst leaving the quadrupole term unchanged. The Hamiltonian for the purely quadrupole term can then be defined as

$$\mathcal{H}(t)/\hbar = \Delta\omega_Q[I_z^2 - \tfrac{1}{3}I(I+1)]S_{zz}(\dot\gamma\tau_d), \tag{3}$$

where I_z is the usual spin angular moment matrix for spin one in the z direction, $\Delta\omega_Q$ is a scaling constant, and S_{zz} is the element of the alignment tensor projected along the magnetic field, as described in Eq. (2).

2. Method

Our approach may be generalised as follows: (i) Subdivide the fluid into representative streamlines, using a Lagrangian (moving fluid element-based) depiction of the flow, (ii) determine, for each streamline, the time-dependence of the rotation matrix which connects the hydrodynamic and Zeeman frames, (iii) calculate the spin Hamiltonian, as a function of time, in each streamline, using a suitable discretisation of time, (iv) calculate the time-dependent NMR signal from each streamline, (v) sum all signals, appropriately weighted, and (vi) Fourier transform to obtain the desired spectrum. Clearly, because of the linearity of the transform, steps (v) and (vi) may be reversed.

Our Couette cell consists of an inner cylinder of radius 2.5 mm and an outer cylinder of radius 3.0 mm, the polymer fluid, being 670 kDa polydimethyl siloxane (PDMS, American polymer Standards, Cincinnati, Ohio) which is contained within the 0.5 mm gap. The introduced deuterated probe molecule was d6-benzene at 5% w/v, a doping level sufficiently small that the polymer rheology was unperturbed. At this level of doping we found the quadrupole splitting constant, $\Delta\omega_Q$, to be 55 Hz. Following selected excitation of the azimuthal sector of interest (see Fig. 2B) a $90_x - t_1 - 180_y - t_1 -$ echo sequence was used, the quadrupole spectrum being obtained by Fourier transforming with respect to the evolution (t_1) domain.

In what follows we lay out our calculation approach following each step in turn. Our numerical simulation uses MATLAB which is well suited to the matrix multiplications inherent in the calculation. Complete spectral evaluations took just a few seconds on a G4 Macintosh computer.

2.1. Step (i)

We divide the fluid in the 0.5 mm gap, into 11 equally spaced elements of different radius, ranging from 2.5 to 3.0 mm. Although we could have chosen to use the measured velocities, we instead choose, for this exercise, to

model the local velocity using the power-law constitutive equation [11] $\sigma_{r,\Phi} = m\dot\gamma^n$, reflecting the fact that the polymer melt is a non-Newtonian fluid, and allowing us to test for the effect of non-uniform shear rates by adjusting the power-law exponent. The power-law model yields an analytic solution for the velocity in our cylindrical Couette geometry. Solving the equation of motion for a power law fluid leads to an explicit expression for the azimuthal component of the velocity field at r:

$$\frac{v_\Phi}{\Omega r_i} = \frac{R(1 - R^{-2/n})}{K(1 - K^{-2/n})} \tag{4}$$

with a corresponding shear rate of

$$\dot\gamma = \frac{2\Omega R^{-2/n}}{n(1 - K^{-2/n})}. \tag{5}$$

Here $K = r_i/r_o$ and $R = r/r_o$, r_i and r_o being the inner and outer cylinder radii, respectively, and the inner cylinder angular velocity is Ω.

2.2. Step (ii)

Obviously, for a given rotation rate Ω, Φ is dependent on the time elapsed following the selective excitation immediately prior to signal acquisition. For each streamline an instantaneous value $\Phi(t)$ is calculated. We choose here the case of an attempt to measure S_{XX}.

2.3. Step (iii)

For each streamline labelled by radius r, and for a given rotation rate Ω, we calculate $\dot\gamma$, and then the components of the alignment tensor, S_{XX}, S_{XY}, and S_{YY}, allowing that these components depend on different local values of $\dot\gamma$ characterising the strength of the interaction. Knowing $\Phi(r,t)$, S_{zz} is calculated from Eq. (2), leading to the Hamiltonian for the quadrupole term and hence to the evolution operator, $U_E(t, \delta t) = \exp[-\frac{i}{\hbar}\mathcal{H}(t)\delta t]$.

2.4. Step (iv)

Starting with an initial density matrix, subsequent to the 90_x RF pulse of the form $\rho(0_+) = I_y$, we evolve $\rho(t)$ using

$$\rho(t + \delta t) = U_E(t, \delta t)\rho(0_+)U_E^\dagger(t, \delta t) \tag{6}$$

and, for each streamline labelled by radius r, the signal contribution is calculated by

$$S(t) = \text{Trace}(I_y\rho(t))\exp(-t/T_2). \tag{7}$$

2.5. Steps (v) and (vi)

The total signal is summed, in our case, because a rectangular slice is excited, each radial contribution having equal weighting. This total signal is then

Fourier-transformed to obtain a frequency spectrum. The calculated deuteron quadrupole splittings are then determined. Note that if no relaxation is included, the discrete Fourier transform truncates the signal, leading to a sinc convolution. This was remedied by multiplying the signal by an exponential damping factor (see Eq. (7)), smoothing out the oscillations in the spectrum. The damping function corresponds to the situation found experimentally: $T_2 \sim \frac{1}{15}$ s. Clearly, features in the spectrum less than about 5 Hz cannot be resolved. This damping factor also means that the signal need only be evaluated up to around 0.4 s using 0.2 ms steps. Note that a non-flowing 'ideal' spectrum can be calculated by examining the signal at the outer wall, where the velocity goes to zero.

3. Results

To gain some insight regarding the role of the rheology in determining the spectral outcome, we have chosen to calculate the spectra using two different power law exponents, 1.0, corresponding to a Newtonian fluid and 0.3, corresponding to a strongly shear thinning fluid. The actual power law exponent of the PDMS melt used in this work is intermediate between these two values, at around 0.5 [12]. First, in Figs. 5 and 6, we show spectra calculated assuming $n = 0.3$, then in Figs. 7 and 8, we show spectra calculated assuming $n = 1.0$. Figs. 5 and 7 show spectra obtained near the outer wall using inner cylinder rotation frequencies of 2, 6, 10, and 20 rad/s, respectively. In this region there is very little flow perturbation and near ideal spectral lineshapes are observed. By contrast, in Figs. 6 and 8, we see the total spectra acquired from fluid across the gap. The spectra are distorted, but to first order, the splittings seem not to be greatly affected, a point we will soon investigate.

Fig. 6. Simulated total spectra obtained right across the gap, the distortions indicating the effects of flow, for a power law exponent of 0.3 and for increasing inner cylinder rotation rates of 2, 6, 10, and 20 rad/s.

Fig. 7. As for Fig. 5 but for $n = 1.0$.

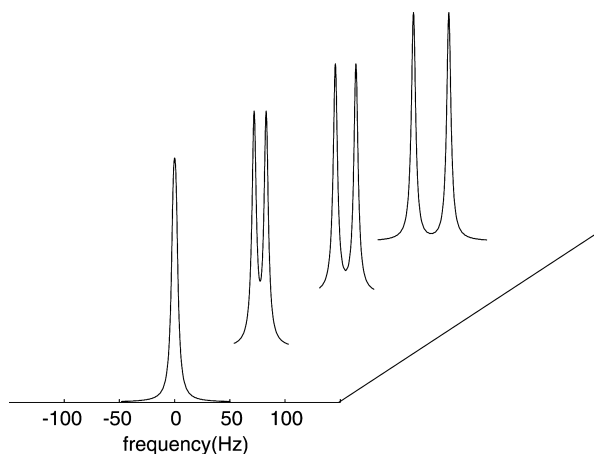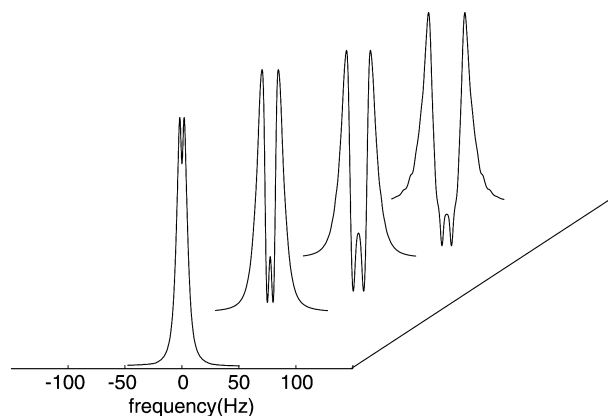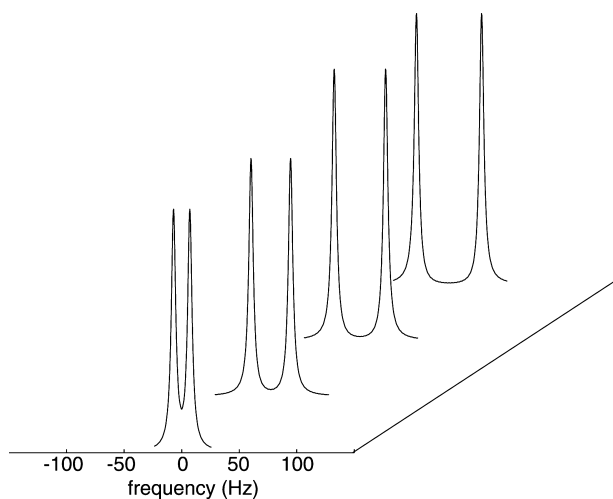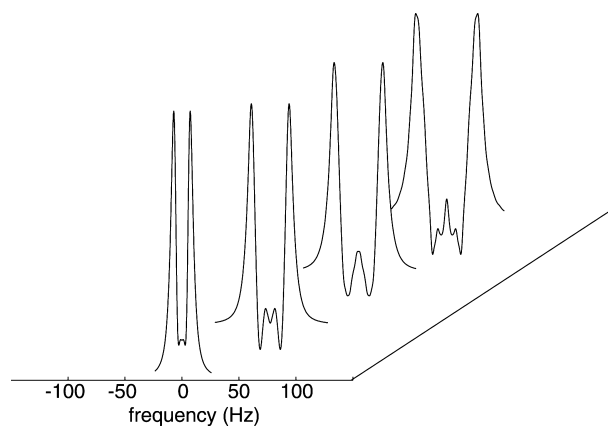Fig. 8. As for Fig. 6 but for $n = 1.0$.

Fig. 5. Simulated spectra obtained near the outer wall where flow influences are minimal, for a power law exponent of 0.3 and for increasing inner cylinder rotation rates of 2, 6, 10, and 20 rad/s.

To compare the calculated spectra with those observed experimentally, we show, by way of example in Fig. 9, a measured spectrum obtained at a rotation speed of 10 rad/s, along with the calculated spectrum,
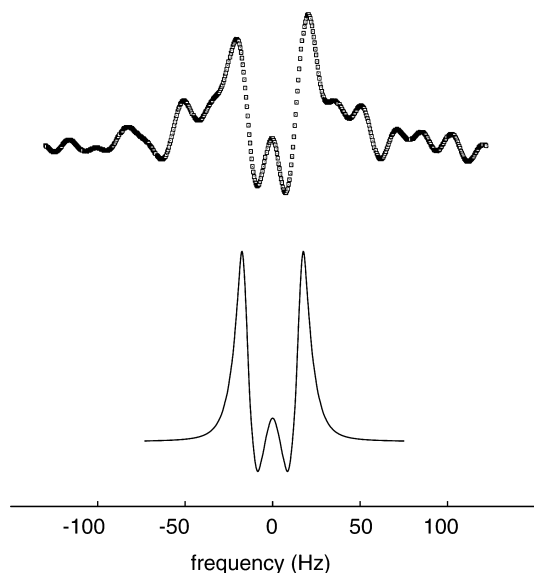
Fig. 9. Comparison of measured and calculated total gap spectra for 10 rad/s inner cylinder rotation speed, using the known power law exponent, $n = 0.5$. Note the appearance of a secondary peak at zero frequency, an artifact of the flow. The measured spectrum was obtained using the 2-D spin echo technique described in [9,12].

at the same rotation speed, assuming the measured power law exponent, $n = 0.5$. The agreement is quite good. Certainly the calculations undertaken here provide an explanation for the unusual secondary peak at zero frequency, making clear that this effect is not due to the presence of another phase for which the quadrupole interaction is zero. That insight alone makes this calculation extremely valuable.

More importantly however, we are interested to know whether the doublet splittings obtained from the entire signal from all fluid elements across the gap are markedly different from those obtained under zero flow, near the outer wall. Fig. 10 compares there, in each case
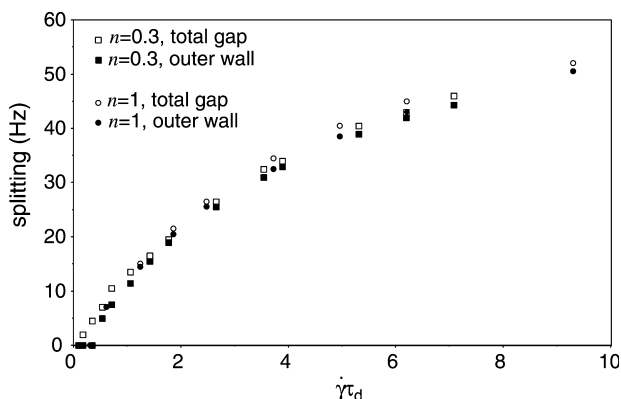

Fig. 10. Comparison of splittings obtained near the outer wall where flow effects are minimal, with those obtained from the integral gap spectrum, both in the case of power law exponents $n = 1.0$ and $n = 0.3$. The agreement is remarkable, when the data are plotted against the known value of $\dot{\gamma}\tau_d$ calculated from the flow at the outer wall.

plotting the the comparative splitting as a function of the dimensionless shear rate (Deborah number, $\dot{\gamma}\tau_d$) calculated at the outer wall. Remarkably the agreement between both outer wall splittings and total gap splittings is excellent, despite the distortions to the spectra obvious in Figs. 6 and 8. Nonetheless, this agreement is dependent on our taking the shear rate as that given by the local velocity gradient at the outer wall. For $n = 1.0$ the difference between inner and outer wall values is not significant, and even for $n = 0.5$, they agree to within a factor of two for the Couette cell geometry used in this work. However for strongly shear thinning fluids it is clear that there may exist a substantial discrepancy between the apparent shear rate (inner wall radius divided by gap separation) and that calculated locally at the outer and inner walls. For such fluids it is clearly important that the outer gap value is used. What Fig. 10 tells us is that this very slowly moving fluid plays a dominant role in the spectrum, probably because the very sharpness of the unperturbed outer wall spectrum causes it to predominate.

Note that we have chosen here to calculate spectral effects in the case of the S_{XX} alignment tensor element only. We have also carried out an analysis of effects on the S_{YY} measurement and note that the behaviours are broadly similar.

4. Conclusions

The calculations contained here give us some confidence in our earlier Rheo-NMR spectroscopy work carried out to determine the alignment tensor for polymers under shear. However, these calculations contain an important warning. When using the deuterium quadrupole interaction to gain insights regarding orientational order under flow, one cannot neglect spectral distortion which may arise when the streamline field causes fluid elements to reorient their hydrodynamic axes during data acquisition. One can gain a rule of thumb indication of these effects by a simple comparison of timescales. However, a full spectral calculation is advisable. In particular, while our simplistic interpretation of peak splittings has proven valid in our work on polymer deformation under shear, some key spectral features have now been explained by our calculations and much greater insight provided regarding how we might interpret our measurements more precisely. These findings have implications for future work concerning extensional flow alignment in Fano flow [22,23], 4-roll mill flow [15], and in contracting tube flow. The methods outlined here should provide a general means of dealing with these effects, a factor which is greatly aided by the facility with which NMR can image the flow field. A knowledge of the local fluid velocities turns out to be crucial in any attempt to calculate spectral effects.

References

[1] A.I. Nakatani, M.D. Poliks, E.T. Samulski, NMR investigation of chain deformation in sheared polymer fluids, Macromolecules 23 (1990) 2686–2692.

[2] Y. Xia, P.T. Callaghan, A study of shear-thinning in high polymer solution using dynamic NMR microscopy, Macromolecules 24 (1991) 4777–4786.

[3] D.A. Grabowski, C. Schmidt, Simultaneous measurement of shear viscosity and director orientation of a side-chain liquid-crystalline polymer by rheo-NMR, Macromolecules 27 (1994) 2632–2634.

[4] P.T. Callaghan, Rheo-NMR: nuclear magnetic resonance and the rheology of complex fluids, Rep. Prog. Phys. 62 (1999) 599–670.

[5] P.T. Callaghan, Rheo-NMR: a new window on the rheology of complex fluids, Encyclopedia Mag. Reson. 9 (2002) 739–750.

[6] M.M. Britton, P.T. Callaghan, M.L. Kilfoil, R.W. Mair, K.M. Owens, NMR velocimetry at microscopic resolution in small rheometric devices, Appl. Magn. Reson. 15 (1998) 287–301.

[7] H. Siebert, D.A. Grabowski, C. Schmidt, Rheo-NMR study of a non-flow-aligning side-chain liquid crystal polymer in nematic solution, Rheol. Acta 36 (1997) 618–627.

[8] P.T. Callaghan, M.L. Kilfoil, E.T. Samulski, Chain deformation for a polymer melt under shear, Phys. Rev. Lett. 81 (1998) 4524–4527.

[9] M.L. Kilfoil, P.T. Callaghan, NMR measurement of the alignment tensor for a polymer melt under strong shearing flow, Macromolecules 33 (2000) 6828–6833.

[10] E. Fischer, P.T. Callaghan, Shear banding and the isotropic to nematic transition in wormlike micelles, Phys. Rev. E 64 (2001) 011501-1–011501-15.

[11] H.A. Barnes, J.J. Hutton, K. Walters, An Introduction to Rheology, Elsevier, Amsterdam, 1989.

[12] R.J. Cormier, M.L. Kilfoil, P.T. Callaghan, Bi-axial deformation of a polymer under shear: NMR test of Doi-Edwards model with convected constraint release, Phys. Rev. E 64 (2001) 051809-1–051809-11.

[13] R.J. Cormier, P.T. Callaghan, Molecular weight dependence of segmental alignment in a sheared polymer melt: a deuterium NMR investigation, J. Chem. Phys. 116 (2002) 10020–10029.

[14] H. Siebert, P. Becker, I. Quijada-Garrido, D.A. Grabowski, C. Schmidt, In situ deuteron NMR investigations of sheared liquid crystalline polymers, Solid State Nucl. Magn. Reson. 22 (2002) 311–326.

[15] R.J. Cormier, C. Schmidt, P.T. Callaghan, Director reorientation of a side-chain liquid crystalline polymer under extensional flow, J. Rheol. 64 (2004) 051809-1–051809-11.

[16] E. Fischer, P.T. Callaghan, Is a birefringence band a shear band?, Europhys. Lett. 50 (2000) 803–809.

[17] W.M. Holmes, M.R. Lpez-Gonzlez, P.T. Callaghan, Shear-induced constraint to amphiphile chain dynamics in wormlike micelles, Europhys. Lett. 66 (2004) 132–138.

[18] M. Doi, S.F. Edwards, Dynamics of concentrated polymer systems, J. Chem. Soc. Faraday Trans. 74 (1978) 1789–1801;
J. Chem. Soc. Faraday Trans. 74 (1978) 1802–1817;
J. Chem. Soc. Faraday Trans. 74 (1978) 1818–1832;
J. Chem. Soc. Faraday Trans. 75 (1979) 35–54.

[19] M. Doi, S.F. Edwards, The Theory of Polymer Dynamics, Oxford, New York, 1986.

[20] M.L. Kilfoil, P.T. Callaghan, Selective storage of magnetization in strongly relaxing spin systems, J. Mag. Reson. B 150 (2001) 110–115.

[21] P.T. Callaghan, Principles of Magnetic Resonance Microscopy, Oxford, NewYork, 1991.

[22] P.T. Callaghan, Y. Xia, Nuclear magnetic resonance imaging and velocimetry of Fano flow, J. Phys. C 16 (2004) 4177–4192.

[23] Y. Xia, P.T. Callaghan, NMR microscopy of tubeless siphon flow, J. Magn. Reson. 164 (2003) 365–368.